

Nanoscale Characterization of Individual Horizontally Aligned Single-Walled Carbon Nanotubes

Gergely Németh,* Dániel Datz, Hajnalka Mária Tóháti, Áron Pekker, Keigo Otsuka, Taiki Inoue, Shigeo Maruyama, and Katalin Kamarás

One of the most challenging tasks in nanotube research is to identify the different electronic types of nanotubes for device fabrication. The implementation of standard spectroscopy techniques at the single-tube level has remained a great task due to small nanotube signal and low spatial resolution. Scattering-type scanning near-field optical microscopy (s-SNOM) yields information on the optical characteristics of the sample with high spatial resolution. We have already demonstrated that this method is able to distinguish between different electronic types of carbon nanotube bundles based on their optical properties in the infrared region. Now we applied the same method to characterize individual horizontally aligned single-walled carbon nanotubes (SWCNTs).

1. Introduction

Single-walled carbon nanotubes (SWCNTs) are still in the focus of research due to their unique physical properties. They are identified by their chirality which dictates the physical structure and electronic properties of the individual species. The selective production of carbon nanotubes is still under intense research for device fabrication like FET arrays,^[1] high performance electronics,^[2] and low noise amplifiers.^[3] The characterization of the individual products of selective growth is an important and difficult task. Different optical methods have been already used to measure individual carbon nanotubes.^[4,5] Nevertheless the small separation between the nanotubes in dense devices require techniques with resolution higher than the diffraction limit. Scattering-type scanning near-field optical microscopy combines high spatial resolution with low detection threshold of optical

properties of materials even on the nanoscale. Unlike earlier works combining far-field spectroscopy and microscopy,^[4,5] these measurements can be performed simultaneously yielding structural and spectroscopic results.

2. Experimental Methods

The scattering-type near-field optical microscope setup provides completely wavelength-independent resolution. It is basically the combination of an atomic force microscope (AFM) and a Michelson interferometer (Figure 1). The AFM part employs standard Si probing tips with metal coating. The end of the tip is

illuminated with a focused laser beam. The light from this laser induces a strong evanescent electromagnetic field which can interact with the sample. The interaction between the near-field and the sample influences the back-scattered light in a way that can be described by a complex scattering coefficient ($\sigma = se^{i\varphi}$). The light scattered back along the illumination path is collected and recorded as the optical signal.

Because only a small part of the scattered light is coming from the tip, the AFM is working in tapping mode to modulate the near-field interaction and the scattered light is analyzed by pseudo-heterodyne detection with the interferometer. Demodulating the acquired signal at higher harmonics (n th) of the tip oscillation frequency (Ω), we can obtain the amplitude (s_n) and the phase (φ_n) of the scattered light.^[6] The higher order we demodulate the signal, the more it will contain from the near-field scattering. In our experiments we used the second (O2) and the third (O3) harmonic demodulation.


Our s-SNOM instrument was produced by Neaspec GmbH. As probing tip we used commercially available Pt-coated Si AFM tips purchased from NanoWorld. The illuminating unit was a tunable quantum cascade laser (QCL) with frequency range 960–1020 cm^{-1} .

3. Sample Preparation

The horizontally aligned SWCNTs were individually grown by CVD technique. After the growing phase, the nanotubes were transferred between gold contacts generated by lithography on a Si/SiO₂ substrate.^[7] Metallic nanotubes were subsequently destroyed by the electrical breakdown technique.^[7–9] Scanning

G. Németh, D. Datz, H. M. Tóháti, Á. Pekker, Prof. K. Kamarás
Institute for Solid State Physics and Optics
Wigner Research Centre for Physics
Hungarian Academy of Sciences
Budapest, Hungary
E-mail: nemeth.gergely@wigner.mta.hu

K. Otsuka, T. Inoue, Prof. S. Maruyama
Department of Mechanical Engineering
School of Engineering
The University of Tokyo
Tokyo, Japan

 The ORCID identification number(s) for the author(s) of this article can be found under <https://doi.org/10.1002/pssb.201700433>.

DOI: 10.1002/pssb.201700433

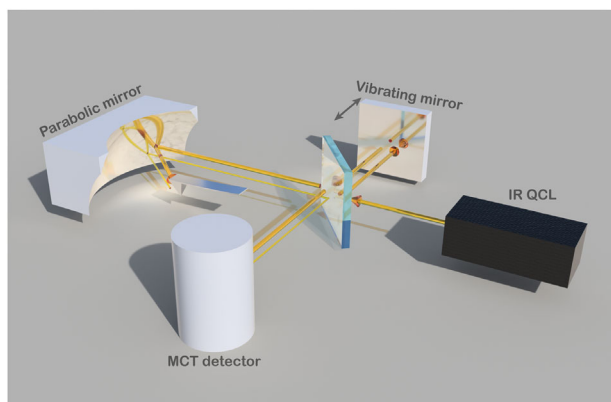


Figure 1. Schematic illustration of the s-SNOM device. The source of the incoming light is an infrared quantum cascade laser (IR QCL) and for the detection we used an MCT detector.

electron microscopy (SEM) images of the samples before and after breaking the metallic nanotubes are shown in **Figure 2**.

4. Optical Properties of CNT Bundles

We performed our s-SNOM measurements in the infrared region between 960 and 1020 cm^{-1} with our QCL laser. In this spectral region the optical properties originate from the excitation of the free charge carriers. The difference between the free carrier density of the semiconducting and metallic nanotubes leads to a difference in the dielectric permittivity. A broad peak in the dielectric function belongs to the zero frequency Drude peak. **Figure 3** presents the complex dielectric permittivity ($\epsilon = \epsilon_1 + i\epsilon_2$) of separated semiconducting and metallic nanotubes. The spectra were acquired from transmittance measurements performed on nanotube thin films and calculated via Kramers–Kronig analysis.^[10]

It has been shown that the near-field phase is proportional to the absorption cross-section (C_{abs}) of the nanoparticle in case of measuring nano-sized systems.^[11] The dielectric permittivity of the particle influences the absorption cross-section so the near-field phase. Because of the different absorption of the two types of nanotubes, we expect distinct near-field phase contrast between the substrate and the two kinds of nanotubes. We note that in s-SNOM measurements we always normalize all data to the signal of the substrate.

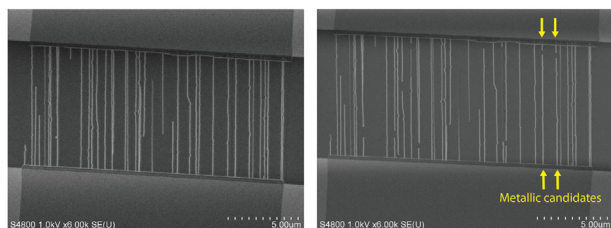


Figure 2. SEM images of the horizontally aligned SWCNT sample, before (left) and after (right) breaking metallic SWCNTs. Two metallic candidates are marked in the area of interest.

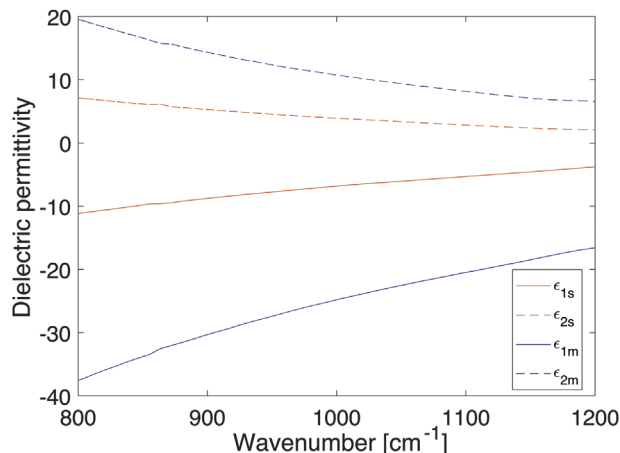


Figure 3. The real (solid) and imaginary part (dashed) of the dielectric function in case of metallic (blue) and semiconducting (red) nanotube samples.

In our previous study, we predicted the difference in the near-field scattered signal in case of metallic or semiconducting nanotube bundles by using the Extended Finite Dipole Model (EFDM).^[12] This model approximates the tip-nanosphere-substrate system with several dipoles. We exchanged the nanosphere to a cylinder by replacing its polarizability to that of a prolate ellipsoid with high aspect ratio.^[13]

The outcome of this calculation^[14] is shown in **Figure 4**. The results verify our expectations. The calculation yields that the metallic nanotubes have higher near-field phase signal relative to the substrate. The near-field phase contrast of the semiconducting nanotubes remains near zero in the range of interest.

5. Results and Discussion

We performed the s-SNOM experiment on the above-mentioned horizontally aligned SWCNT sample. The nanotubes are located

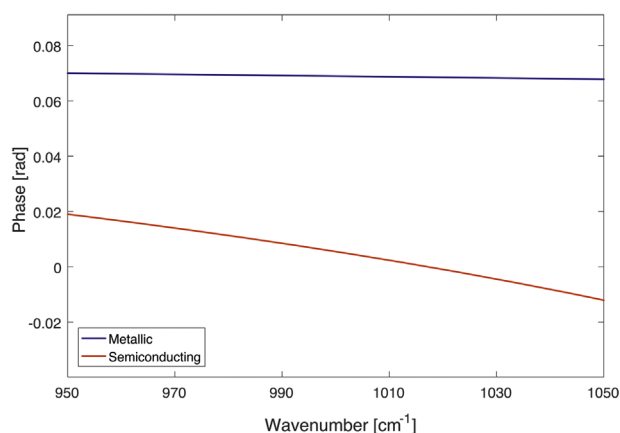


Figure 4. The result of the EFDM calculation for third harmonic demodulated (O3) near-field phase signal for metallic (blue) and semiconducting (red) nanotube bundles with diameter of 4 nm. All data were normalized to the substrate.

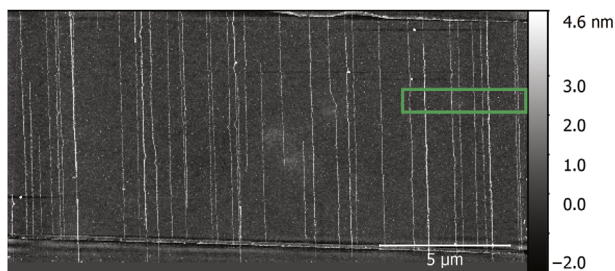


Figure 5. AFM topography image of the horizontally aligned nanotube sample. The green box represents the region of interest for the high resolution measurements which has two metallic nanotube candidates among several semiconducting nanotubes.

between the gold contacts on a SiO_2 substrate. The optical properties of the substrate are crucial for the measurement, as the substrate has to provide appreciable near-field signal in order to have the appropriate coupling between the nanoparticle and the tip. Fortunately SiO_2 has almost as high near-field scattering as Si in this infrared region.

The AFM topography map of the sample can be seen in **Figure 5**. For high resolution s-SNOM measurements, we chose a clean area (indicated by the green rectangle) where the nanotubes are properly separated to measure them individually. The chosen area contains two metallic nanotube candidates.

The outcome of the high resolution third-harmonic demodulated measurements at 985 cm^{-1} is presented in **Figure 6**. The upper map is the corresponding AFM topography. The blue boxes indicate the metallic nanotube candidates. The diameter of these metallic tubes are ≈ 3 and 1.7 nm . The third-harmonic demodulated phase map (φ_{O3}) was acquired simultaneously and is presented in the lower part of **Figure 6**. The phase responses of the individual nanotubes are similar to those of the bundles. We find that the two metallic candidates give the highest phase response, with the larger tube showing $\varphi_{O3} = 0.168\text{ [rad]}$ and the smaller $\varphi_{O3} = 0.132\text{ [rad]}$. It is very important to note that in general the size of the nanoparticle influences the near-field contrast between the substrate and the particle.^[15]

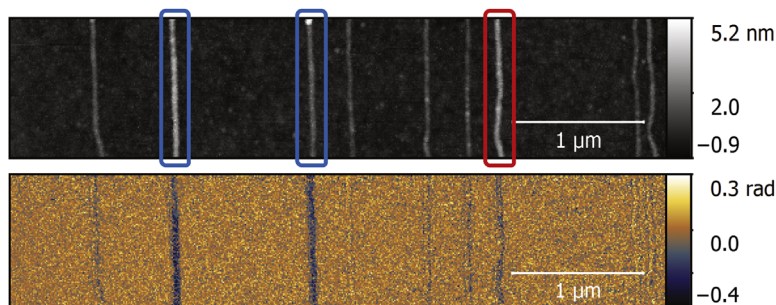


Figure 6. AFM topography image of the chosen area for high resolution s-SNOM measurements (above) and the O_3 near-field phase map at 985 cm^{-1} of the same area (below). The blue boxes indicate the metallic nanotube candidates. The red box stands for the largest semiconducting nanotube.

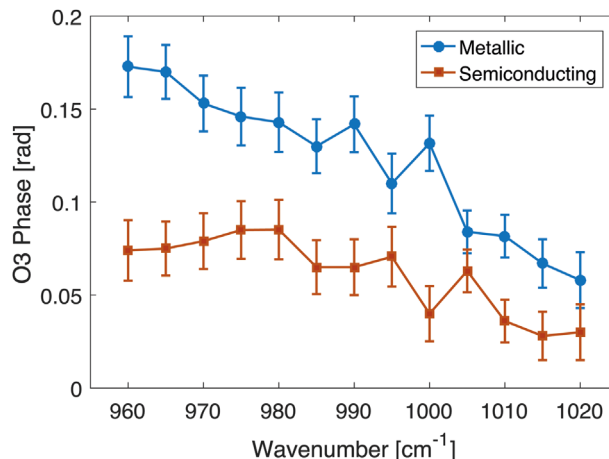


Figure 7. Third-harmonic demodulated (O_3) near-field phase spectra of a semiconducting (red) and metallic (blue) carbon nanotube.

The O_3 phase map also shows that the largest semiconducting tube (2.5 nm) (red box) exhibits a lower phase signal than the smallest metallic one. Based on these observations we can declare that all nanotubes in this area with lower phase contrast than the 1.7 nm metallic carbon nanotube, are semiconducting ones.

We also examined the spectral behavior of these individual nanotubes. **Figure 7** shows the result of these measurements. We can conclude from the spectra that the frequency dependence of the near-field phase signal follows that of the imaginary part of the dielectric function.

We find that at higher wavenumbers (1025 cm^{-1}) the phase of the semiconducting nanotubes is obstructed by the noise, but the phase of the metallic ones is still detectable.

6. Conclusions

In our study, we found that near-field infrared imaging of individual SWCNTs is possible even on a SiO_2 substrate. We proved that the electrical breakdown technique destroys partially only the metallic nanotubes. The spectroscopic study verifies that the near-field phase is connected with the imaginary part of the dielectric function.

Acknowledgments

Á.P. gratefully acknowledges support from the János Bolyai Fellowship of the Hungarian Academy of Sciences and from the National Research, Development and Innovation Office – NKFIH PD 121320. Research was supported by the Hungarian National Research Fund (OTKA) No. SNN 118012.

Conflict of Interest

The authors declare no conflict of interest.

Keywords

alignment, carbon nanotubes, nanomaterials, scanning near-field optical microscopy

Received: August 10, 2017

Revised: October 15, 2017

Published online: November 6, 2017

-
- [1] S. J. Kang, C. Kocabas, T. Ozel, M. Shim, N. Pimparka, M. A. Alam, S. V. Rotkin, J. A. Rogers, *Nature Nanotechnol.* **2007**, 2, 230.
- [2] D. Sun, M. Y. Timmermans, Y. Tian, A. G. Nasibulin, E. I. Kauppinen, S. Kishimoto, T. Mizutani, Y. Ohno, *Nature Nanotechnol.* **2011**, 6, 156.
- [3] K. Parrish, Carbon nanotube transistors for a low noise amplifier: Feasibility and future, **2010**.
- [4] M. Y. Sfeir, T. Beetz, F. Wang, L. Huang, X. M. H. Huang, M. Huang, J. Hone, S. O'Brien, J. A. Misewich, T. F. Heinz, L. Wu, Y. Zhu, L. E. Brus, *Science* **2006**, 312, 554.
- [5] T. Michel, M. Paillet, D. Nakabayashi, M. Picher, V. Jourdain, J. C. Meyer, A. A. Zahab, J. L. Sauvajol, *Phys. Rev. B* **2009**, 80, 245416.
- [6] R. Hillenbrand, F. Keilmann, *Appl. Phys. Lett.* **2006**, 89, 101124.
- [7] P. G. Collins, M. S. Arnold, P. Avouris, *Science* **2001**, 292, 706.
- [8] K. Otsuka, T. Inoue, S. Chiashi, S. Maruyama, *Nanoscale* **2014**, 6, 8831.
- [9] K. Otsuka, T. Inoue, Y. Shimomura, S. Chiashi, S. Maruyama, *Nanoscale* **2016**, 8, 16363.
- [10] H. M. Tóhádi, Á. Pekker, B. Á. Pataki, Z. Szekrényes, K. Kamarás, *Eur. Phys. J. B* **2014**, 87, 126.
- [11] J. M. Stiegler, Y. Abate, A. Cvitkovicand, Y. E. Romanyuk, A. J. Huber, S. R. Leone, R. Hillenbrand, *ACS Nano* **2011**, 5, 6494.
- [12] N. Ocelic, Quantitative Near-Field Phonon-Polariton Spectroscopy, *Ph.D. Thesis*, Technical University Munich, **2007**.
- [13] J. Venermo, A. Sihvola, *J. Electrostat.* **2005**, 63, 101.
- [14] G. Németh, D. Datz, H. M. Tóhádi, Á. Pekker, K. Kamarás, *Phys. Status Solidi B* **2016**, 253, 2413.
- [15] A. Cvitkovic, Substrate-Enhanced Scattering-Type Scanning Near-Field Infrared Microscopy of Nanoparticles, *Ph.D. Thesis*, Technical University Munich, **2009**.